

Characterisation of ceria supported chromia catalysts

R.P. Viswanath*, P. Wilson

Department of Chemistry, Indian Institute of Technology, Chennai 600036, Tamilnadu, India

Received 26 August 1999; received in revised form 17 November 1999; accepted 3 December 1999

Abstract

A series of ceria supported chromia catalysts of different loading were prepared and the effect of support in stabilising various chemical and molecular states of chromium with the calcination temperature were studied. XRD results showed that the chromia phase is randomly dispersed, disordered, and the crystallite size may be smaller than the detection limit. BET surface area and pore volume results suggested some plugging of pores on the support by chromia phase. EGA analysis suggested the existence of the surface heterogeneity involving weakly and strongly chemisorbed CO₂. EGA and NIR DRS studies revealed the bulk-like behaviour in the catalysts having chromia loading of more than 5 wt.%. EGA, FTIR and UV–VIS–DRS studies supported the formation of anchored surface chromium species. Moreover, the nature of molecular states of chromium and the coordinative environment under various thermal conditions were investigated using FTIR and UV–VIS–DRS techniques. © 2000 Elsevier Science B.V. All rights reserved.

Keywords: Surface chromia; Ceria support; Oxide–oxide interaction

1. Introduction

The industrial importance of supported chromium oxide catalysts has motivated a large number of studies relating to its specific surface properties and catalytic behaviour. With the advancements of the physico-chemical techniques in the recent years a detailed characterisations of these systems are being carried out to understand the true picture of the chemical and molecular states of chromia stabilised over various supports and results are well documented in the literature [1–8]. Although these systems are extensively studied, there are still some points of disagreements about the surface structures of chromium oxide species stabilised on various supports and about the true nature of these species in various catalytic processes [9]. These systems find their appli-

cations in polymerisation reactions and many catalysed reactions such as dehydrogenation of alkanes, dehydrocyclisation, catalytic reforming, hydrodesulphurisation and partial oxidation of hydrocarbons [1].

Chromium oxides can be supported by the deposition of precursors on a given support using impregnation or coprecipitation methods, followed by calcination in dry air depending upon the nature of the support, at temperatures greater than 573 K. This results in the formation of various chromium oxide species on the support surface, due to the interaction of the chromium phase with the surface hydroxyls of the support phase [10]. The above interaction strongly affects the molecular and chemical states of surface chromia phase, and thus the catalytic behaviour. The overall catalytic activity and selectivity are dependent on the dispersion of the surface metal oxide species [2].

* Corresponding author.

The modifications of the chemical and molecular states of chromium species on a given support depend on the calcination temperature and atmospheric conditions [6]. Hence, a temperature-programmed study of the chromium species on various supports under different atmospheric conditions would offer us a picture as to how the chemical and molecular environments of the chromium species are dependent on the experimental conditions employed. Hill and Ohlmann [11] and Ruddick et al. [12] have reported a temperature programmed study of silica-supported chromia with different chromia precursor materials.

Various oxides such as SiO_2 , Al_2O_3 and ZrO_2 have been employed as supports for chromia. Their physico-chemical characterisations were carried out using a variety of surface techniques [1,3,6,8,13]. From the recent past TiO_2 has been studied as a support for chromia. Its catalytic properties were examined for the selective catalytic reduction of NO_x , as it is found to stabilise amorphous chromia on its surface [3].

Oxide–oxide interactions are considered as a separate group of phenomena occurring at the catalyst surface during the stages of both preparation and use. In 1993, Chernavskii and Lunin reviewed [14] on oxide–oxide interaction in supported Ni, Co and Fe oxide catalysts, where they have discussed the possible interaction of the above mentioned metal oxides with various supports such as TiO_2 , Al_2O_3 and SiO_2 . There are also reports on the study of ceria supported CuO and V_2O_5 [15,16].

Over the past several years, cerium oxide and CeO_2 -containing materials have come under intense scrutiny as catalysts, structural and electronic promoters and as supports for metals such as Pt, Pd, Rh, Ru, Ir and Ni [17–19]. In recent years, the utilisation of ceria as an essential component in three way catalysts for automotive pollution control has stimulated a significant interest in exploring its properties for various catalytic applications [20]. The presence of cerium oxide as a support is known to improve the dispersion of the active component via formation of M–O surface complexes in calcined samples [21].

To the best of our knowledge, the studies carried out so far on ceria supported chromia catalysts are very limited. There has been a report on the study of isobutane dehydrogenation using the above system [22]. In the present study, an attempt has been made to pre-

pare a series of ceria-supported chromia catalysts of different loadings and to study the thermal decomposition behaviour of the supported chromia phase and the effect of support in stabilising various chemical and molecular states of chromia with the calcination temperature. The investigation of the thermal decomposition behaviour of the bulk and supported chromia over ceria support was carried out using X-ray diffraction (XRD) and evolved gas analysis (EGA), with the aim of determining the degree of active phase support interaction. The textural properties of the above system were studied using BET surface area measurements as a function of chromia loading. The influence of oxide–oxide interactions on the chemical and molecular states of chromia was established by FTIR and UV–VIS–DRS techniques.

2. Experimental

2.1. Catalyst preparation

All the catalysts were prepared by an impregnation method using commercial ceria as support and aqueous CrO_3 as precursor. The impregnated catalysts were dried at 393 K for 12 h and calcined at 573 K for 2 h. The dried samples will be hereafter referred to as the *fresh* catalysts. The ceria-supported chromia catalysts prepared will be denoted as CrCe X, where X is the loading expressed in wt.% of chromia.

2.2. Chemical analysis

The chemical analysis of Cr VI was carried out based on the property that water removes CrO_3 from the support [4]. The estimation was carried out spectrophotometrically at λ_{max} of 350 nm; this is reported to be a highly suitable method for determining chromium bound to the support in +6 oxidation state [23].

For both fresh and calcined samples, the estimation was carried out in three stages. About 0.25 g of the catalyst sample was first leached with about 20 ml of distilled water by stirring for about 30 min and then decanting the clear solution to remove any free chromia present on the surface. The leaching in all the cases was performed repeatedly for at least three times, till the solution becomes colourless. Then the extract

I was made up to a known volume to be estimated for the free chromia content.

The residue thus left behind was further digested with 20 ml of dil. H_2SO_4 to remove the chromium species bound to the support surface strongly as Cr^{6+} . Thus after repeated washings, the estimation was carried out for anchored Cr^{6+} species content. Since acid digestion involves heat treatment, possibly the Cr^{3+} species would also come out along with anchored Cr^{6+} species. Hence, another portion of the extract II was further heated with $\text{NaOH}/\text{H}_2\text{O}_2$ to oxidise the Cr^{3+} species in the extract till the effervescence ceases in order to ensure the complete decomposition of H_2O_2 from the extract. The extract III thus obtained was then acidified with dil. H_2SO_4 and its total amounts of anchored Cr^{6+} and Cr^{3+} species content were estimated. The difference in the amount of Cr^{6+} in the peroxide-treated (extract III) and acid-leached solution (extract II) would result in the amount of Cr^{3+} species present.

2.3. X-ray diffraction (XRD)

X-ray diffraction measurements were carried out on a Rigaku, miniflex diffractometer in the range $5\text{--}90^\circ/\text{min}$ (chart speed $20\text{ mm}/\text{min}$) using $\text{Co K}\alpha$ ($\lambda=1.7902$) radiation filtered through a Ni filter for bulk CrO_3 , Cr_2O_3 , CeO_2 and for supported chromia catalyst samples of loading 8 wt.%, calcined at 773, 873, 973, 1073 and 1173 K.

2.4. Surface area and pore volume

The BET surface area and pore volume were calculated for pure ceria and supported chromium catalysts of various loadings.

2.5. Evolved gas analysis (EGA)

The temperature programmed study was carried out between 323 and 673 K by monitoring the evolved

gases using a quadrupole mass filter (Balzers GAM 442 Gas Analyser) at a scanning rate of $10^\circ/\text{cycle}$, with the extreme sensitivity and resolution enabling one to trace even a species having an ion current as low as 10^{-14} A.

2.6. FTIR spectroscopy

FTIR spectroscopic experiments were undertaken in a Perkin–Elmer spectrometer accumulating 10 scans at 4 cm^{-1} resolution for fresh and calcined samples of supported chromia catalysts. In situ FTIR study was also carried out under a pressure of the order of 10^{-6} Torr at various temperatures.

2.7. UV–VIS–NIR diffuse reflectance spectroscopy

UV–VIS–NIR diffuse reflectance spectroscopic profiles were recorded for fresh and calcined samples of supported chromium catalysts, and for Cr_2O_3 using a Cary 5E UV–VIS–NIR spectrophotometer between 200 and 2000 nm.

3. Results and discussion

The chemical analysis carried out for fresh and calcined samples of CrCe 5 exhibited how the distribution of various chromia species on the support surface gets modified as a result of interaction, on calcining at 573 K, for 2 h. Results are shown in Table 1.

The total amount of chromia extracted from the fresh sample is referred to as total chromia and was found to be 4.3%. It is evident from the chemical analysis that the free chromia content of the calcined sample is much less (7.6%) and the anchored chromia species is present in reasonably higher amounts (56%) in comparison with the fresh sample. This confirms the possibility of the formation of surface anchored chromia species as a result of the interaction between the chromia and the support phase on calcination. The

Table 1
Distribution of various surface chromia species on fresh and calcined samples

S. No.	Sample	Water leached (free chromia, %), I	Acid digested, II	$\text{NaOH}/$ H_2O_2 , III	Total chromia, T	Anchored Cr^{6+} (%), $\text{II}/T \times 100$	Cr^{3+} Species (%), $\text{III}-\text{II}/T \times 100$
1	Fresh	4.1 (95)	0.157	0.24	4.3	3.6	1.9
2	Calcined	0.33 (7.7)	2.407	3.27	3.6	56	20

fact that still a small quantity of Cr^{6+} (3.6%) is stabilised even in fresh samples may be ascribed to the longer period of drying (12 h) involved in the process of preparation. A similar explanation can also be extended to the presence of a small amount of Cr^{3+} species (1.9%) observed for fresh samples.

The amount of Cr^{3+} species determined indirectly from the difference in chromia content corresponding to extract III ($\text{NaOH}/\text{H}_2\text{O}_2$ treated) and extract II (acid leached) includes the distribution of various Cr^{3+} species such as microcrystalline, isolated Cr^{3+} and amorphous. It is not feasible to distinguish and quantify the same with chemical analysis. Thus, the 20% of the total chromia present as Cr^{3+} species on the surface of the sample calcined at 573 K shows that a fraction of free chromia has undergone thermal reduction upon calcination.

The total amount of chromia extractable in the calcined sample is 84% with reference to the uncalcined sample. The chemistry of the unleached chromia species, calculated from the above procedure to be 16%, is at present not clearly understood. Further investigations are in progress to account for the distribution of various chromia species on the

Table 2
Effect of calcination on the XRD pattern of bulk and supported CrO_3

S. No	Calcination temperature (K)	Bulk CrO_3	CrCe 8
1	673	CrO_3	CeO_2 phase
2	773	$\alpha\text{-Cr}_2\text{O}_3$	CeO_2 phase
3	873	$\alpha\text{-Cr}_2\text{O}_3$	CeO_2 phase
4	973	$\alpha\text{-Cr}_2\text{O}_3$	CeO_2 phase
5	1073	$\alpha\text{-Cr}_2\text{O}_3$	CeO_2 phase
6	1173	$\alpha\text{-Cr}_2\text{O}_3$	CeO_2 phase

surface, especially with reference to the unleached chromia.

Table 2 shows the phases identified from the XRD measurements. Examination of the XRD pattern for the bulk chromia shows the presence of crystalline CrO_3 at temperatures lower than 773 K. It was observed that, as the calcination temperature increases from 773 to 1173 K, the growth of phases corresponding to the formation of $\alpha\text{-Cr}_2\text{O}_3$ took place as a result of crystallisation. But the XRD patterns of CrCe 8 calcined at the aforementioned temperatures show only the ceria phase till the calcination temperature of 1173 K. These are shown in Fig. 1. However, the

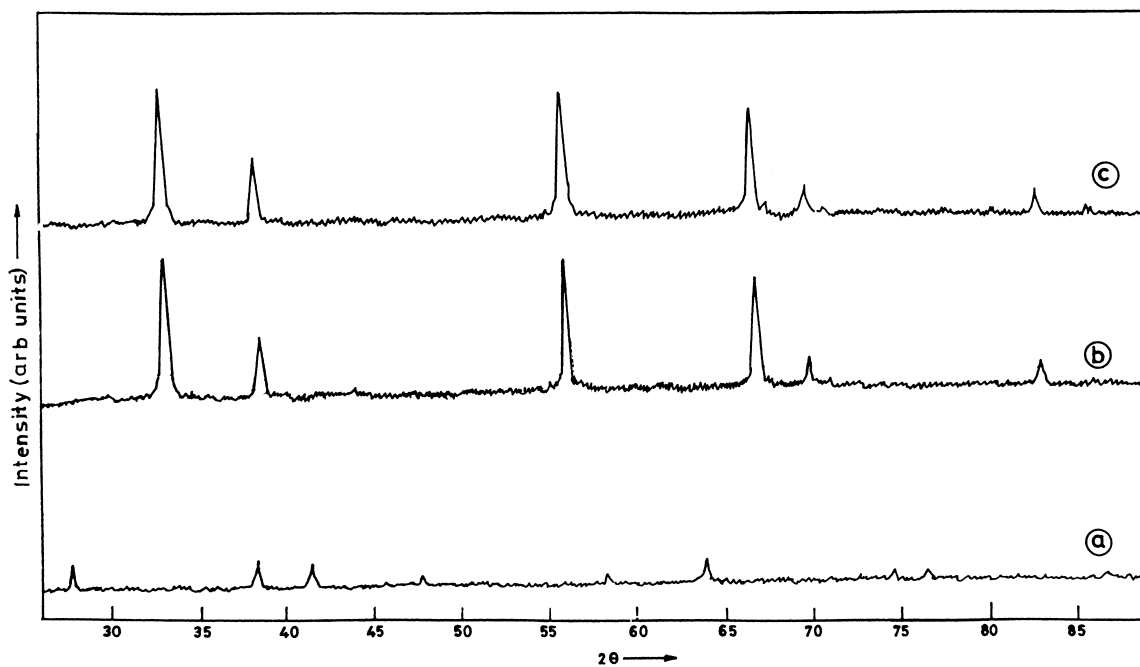


Fig. 1. XRD pattern of (a) Bulk Cr_2O_3 ; (b) Bulk CeO_2 ; (c) CrCe 8, calcined at 1173 K, 2 h.

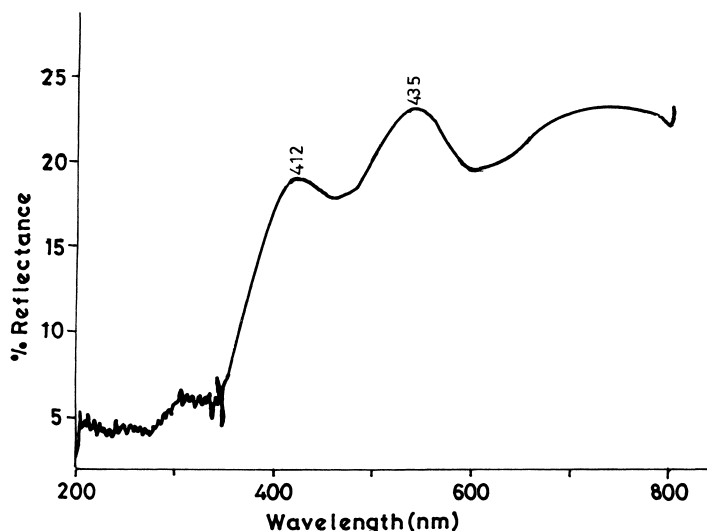


Fig. 2. UV–VIS–DRS profile of CrCe 8, calcined at 673 K, 2 h.

green colour of the sample and the characteristic bands of Cr^{3+} shown in UV–VIS–DRS profile (Fig. 2) indicates the presence of Cr_2O_3 even at 673 K. TG and DSC measurements carried out for bulk CrO_3 showed that it decomposes completely to $\alpha\text{-Cr}_2\text{O}_3$ between 773 and 806 K. Thus the absence of chromia phase in the diffraction pattern for the supported catalysts may be attributed to the fact that the chromium species are randomly dispersed, disordered, and the crystallite size may be smaller than the detection limit. The same pattern is observed even after changing the X-ray source to Cu $\text{K}\alpha$ under the above conditions. The fact that one could not trace any crystallising material of chromia even on increasing the chromia content to 16 wt.% substantiates the postulate that X-ray amorphous microcrystals of chromia phase are stabilised on the given support.

Table 3 gives the data on the surface area and pore volume of supported chromium catalysts. The deposi-

tion of chromium species on CeO_2 support caused a decrease in both specific surface area and pore specific volume of the support. Thus, the decreases in both its specific surface area and pore specific volume may be attributed to the plugging of pores on the support by chromia phase [5].

In Fig. 3(a) and (b) are shown the evolved gas profiles of the bulk CrO_3 and CrCe 8 catalyst. EGA shows a variety of species evolved during the temperature-programmed study. Evolution of species corresponding to mass 44 (Fig. 3d) is ascribed to the adsorption of CO_2 through several mechanisms leading to different carbonate-like species. Due to its basic character, ceria strongly binds carbonate entities even without performing any CO or CO_2 adsorption experiments [21]. The fact that the desorption of CO_2 is observed in stages at 513, 573 and 603 K, respectively, whereas a gradual desorption of CO_2 was witnessed in the above mentioned temperature range for pure ceria (Fig. 3c) suggests the existence of the some surface heterogeneity involving weakly and strongly chemisorbed CO_2 . Thus the species corresponding to mass 44 evolving quickly at lower temperature can be ascribed to the weakly chemisorbed CO_2 and that evolving at higher temperature to the one which is strongly chemisorbed. Presence of CO_2 can further be evidenced from the band at 1383 cm^{-1} in FTIR spectrum (Fig. 4).

Table 3
Specific surface area and pore volume of CrCe catalysts

Sample	S_{BET} (m^2/g)	Pore volume ($10^{-3}\text{ cm}^3/\text{g}$)
CeO_2	17.57	9.94
CrCe 0.67	7.85	4.36
CrCe 1.29	8.88	4.64
CrCe 3.80	9.05	4.89

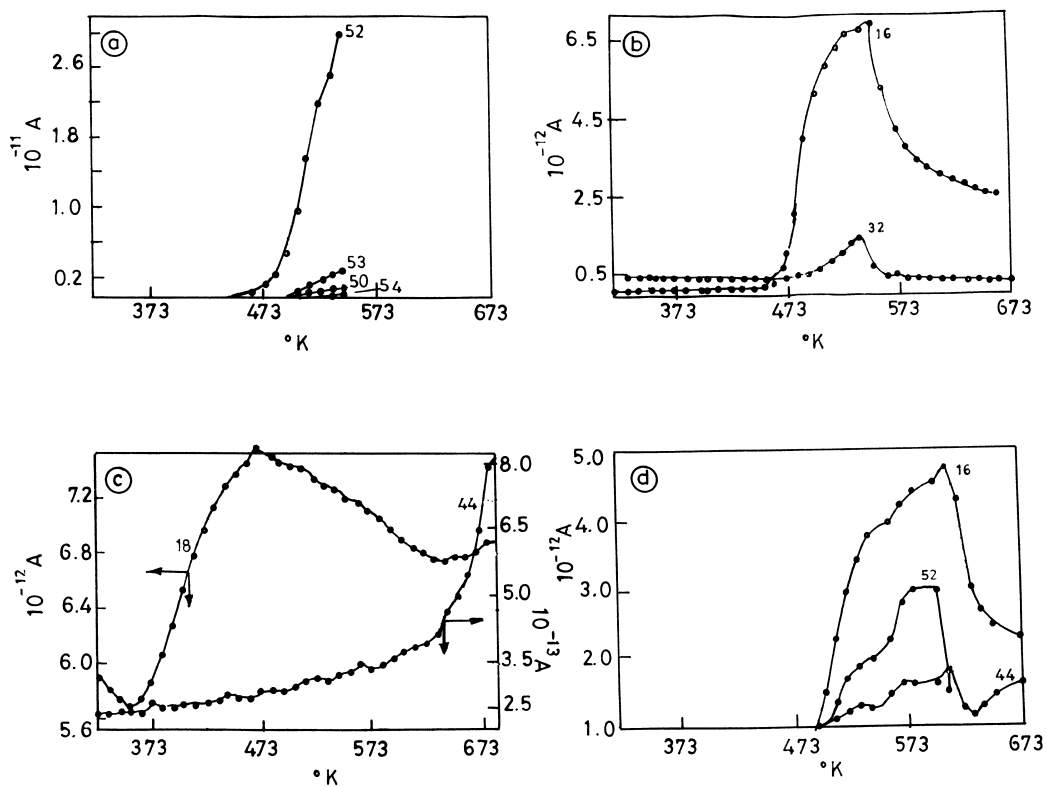


Fig. 3. (a and b) EGA profile of bulk CrO_3 ; (c) EGA profile of pure CeO_2 ; (d) EGA profile of CrCe 8 (fresh).

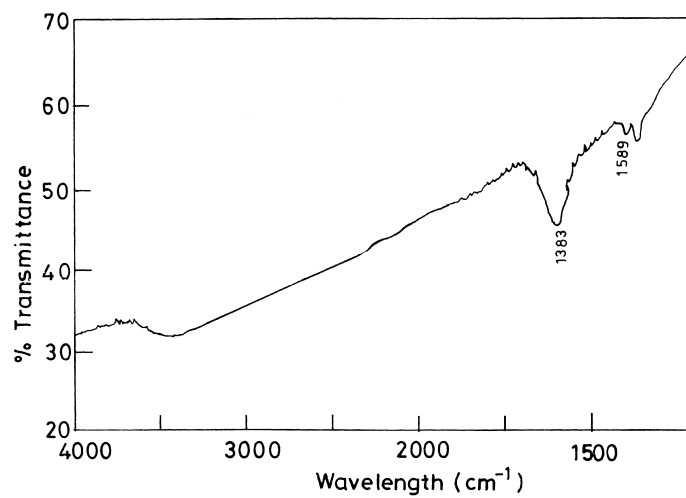


Fig. 4. FTIR spectrum of CrCe 8, calcined at 573 K, 2h.

The peak observed between 473 and 543 K corresponding to mass 52 for bulk chromia (Fig. 3a) is assigned to chromium ions detected as Cr^+ due to the decomposition of CrO_3 . Additional support for the decomposition of bulk chromia can be found from the evolution of atomic and molecular oxygen species between 473 and 543 K (Fig. 3b) with the corresponding peaks observed at mass 16 and 32, respectively. It is also known that the melting point of bulk chromia is 473 K. Bulk chromia is more thermally unstable than the supported chromia and begins to decompose into Cr_2O_3 and O_2 at 533 K [4]. TG and DSC studies carried out in our laboratory [24] for the bulk CrO_3 also agrees well with the literature report [4].

The similar patterns of evolution observed for CrCe 8 in (Fig. 3d) for species of mass 52, 16 and 44 under the temperature range studied suggest that CO_2 is adsorbed mostly on coordinatively unsaturated chromium sites on the surface. The same conclusion can further be justified by the band observed at 1025 cm^{-1} [10] in FTIR profile shown in Fig. 6. It is evident from the EGA profile of pure ceria that considerable desorption of CO_2 from its surface occurs only above 603 K and hence it is concluded that the desorption of CO_2 occurring at lower temperatures is due to that adsorbed on chromium sites in various modes. Moreover, the band observed at 1589 cm^{-1} is ascribed to the non-dissociatively adsorbed water; this in turn further substantiates the presence of coordinatively unsaturated chromium sites.

The EGA profile for the fresh sample of CrCe 8 shows the evolution of species corresponding to mass 52, which implies the manifestation of bulk-like behaviour (Fig. 3d). On the other hand, for the same sample calcined at 573 K, the peak corresponding to mass 52 is absent, suggesting the presence of anchored surface chromium species, formed as a result of the interaction between chromia and the support phase. It is also noted that the fresh sample of CrCe 5 catalyst did not show the evolution of species of mass 52, indicating that the bulk-like behaviour is more pronounced when the loading of chromia exceeds 5 wt.%. Upon heating, the supported chromium oxide species do not decompose into O_2 and Cr_2O_3 (like bulk chromia) at least for the lower loading, but are anchored by an esterification reaction with the hydroxyl groups of the inorganic oxide, resulting in the formation of surface chromium species. Thus, one can conclude that the

surface chromium (VI) species are stabilised on the CeO_2 support upon calcination as a result of effective interaction between CrO_3 and the support phase. Evidence can also be had from differential thermal analysis study for a supported chromium sample reported elsewhere [24]. The endothermic peaks at 373 and 493 K indicate the removal of water in two stages; first the physisorbed one, followed by the water of condensation. The removal of water of condensation is due to the esterification reaction through dehydroxylation occurring between surface hydroxyl groups of active and the support phase [4,10].

NIR DRS also complements the view that the 5% chromia is the threshold amount, beyond which the growth of the bulk chromia begins. Fig. 5 shows the NIR DRS profile of the ceria-supported chromium catalysts of various loading values and of pure ceria. The diffused bands observed around 1363, 1657 and 1859 nm in the NIR region of the DRS profile are attributed to the presence of surface hydroxyl groups [8]. Fig. 5a indicates the presence of surface hydroxyl groups on the ceria support alone. With the increase in chromia content, the intensity of the band decreases owing to consumption of OH groups as a result of dehydroxylation occurring between active chromia and the support phase. When the chromia content approaches 5 wt.%, dehydroxylation is almost completed. This along with the results of evolved gas analysis suggests that the formation of surface chromates gets completed when the chromia content of the catalyst approaches the range 4–5 wt.%. Beyond this content the given support is unable to stabilise the CrO_3 phase on its surface as a result of which the bulk-like behaviour of chromia is exhibited.

The FTIR spectrum recorded for the sample of CrCe 10% is given in Fig. 6. The spectrum for the fresh sample (Fig. 6a) shows bands at 960 and 945 cm^{-1} corresponding to tetrahedrally coordinated chromium centres of tetrameric chromate species ($\text{Cr}^{6+}=\text{O}$) [25]. The weak band observed at 890 cm^{-1} is assigned to the stretching mode of Cr–O–Cr chains, indicating the presence of polymeric chromium species. The intense band observed at 907 cm^{-1} is ascribed to the stretching mode of $\text{Cr}^{6+}=\text{O}$ groups. The IR bands observed in the 1130 – 830 cm^{-1} region are generally attributed to the chromium–oxygen groups. The higher frequency region between 1050 and 1000 cm^{-1} is typical of chromium–oxygen groups having a larger

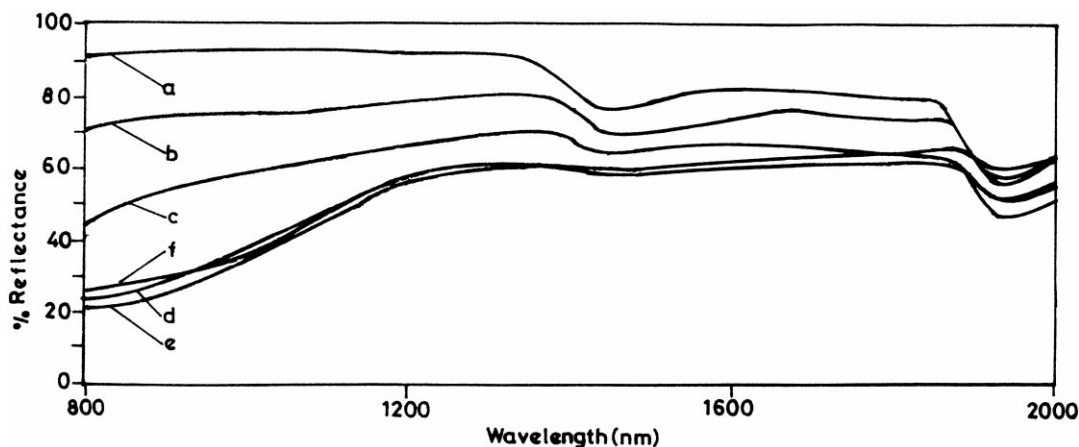


Fig. 5. NIR-DRS profiles of CrCe catalysts, calcined at 573 K, 2 h; (a) CeO₂; (b) CrCe 1; (c) CrCe 2; (d) CrCe 5; (e) CrCe 8; (f) CrCe 10.

double bond character. The broadness of the bands and the lower frequency region between 950 and 830 cm⁻¹ are typical of chromium–oxygen groups having a lower double bond character and of Cr–O–Cr chains (symmetric stretching only) [25,26]. Under

ambient conditions, the surface of the oxide support becomes hydrated and the surface chromium oxide over layer is essentially in an aqueous medium. The following successive equilibria have been proposed for the behaviour of Cr (VI) under various acidic conditions in aqueous solutions.

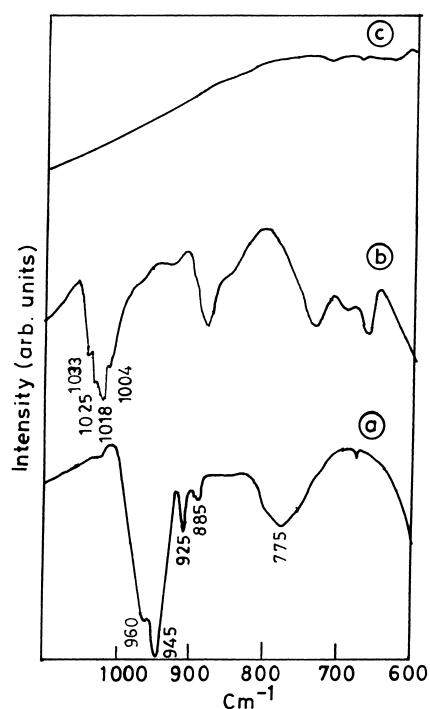
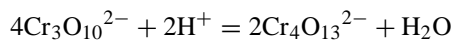
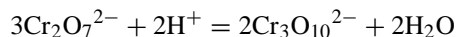
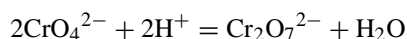


Fig. 6. FTIR spectra of CrCe 10 catalyst, calcined at (a) 393 K; (b) 573 K; (c) 673 K.

A similar model proposed by Deo and Wachs [7] helps one to predict the molecular structure of supported metal oxides under ambient conditions. It was found that, under hydrated conditions, the molecular structure is determined by the net pH at which the surface possesses zero charge (PZC, point of zero charge) and by the surface coverage. The pH at PZC for a given support decreases as the Cr loading increases. Consequently, for the ceria-supported chromia sample having higher chromium content (CrCe 10) under hydrated (fresh) conditions, chromium oxide is more polymerised.

The pattern observed for CrCe 10 calcined at 573 K for 2 h in FTIR spectrum (Fig. 6b) contains a group of bands at 1033, 1018 cm⁻¹ and a shoulder at 1004 cm⁻¹ and are attributed to the chromium–oxygen groups having a larger double bond character [25,26]. This can clearly be perceived as a shift in the position of bands to the higher frequency side in comparison

to the fresh one (Fig. 6a). Further, it can be referred from the literature that Cr=O stretching modes are very sensitive to the surrounding [13]. Thus, it is reasonable to conclude that surface rearrangement of molecular species in the sample calcined at 573 K for 2 h has resulted in the development of different environment in the molecular structure of chromia species. This phenomenon can further be substantiated by considering the shift of IR bands to the higher frequency region on calcination, being caused by the interaction of the chromate species with the support. The interaction between the oxygen group of the CrO_4^{2-} ion and the support surface will decrease the negative charge on the chromate ion. Since the chromate and dichromate ions can be described as O^{2-} species stabilised by one or two CrO_3 units, it follows that in the case of CrO_4^{2-} the doubly negative charge is delocalised over the whole CrO_4^{2-} group, whereas for $\text{Cr}_2\text{O}_7^{2-}$ only a single negative charge is available per CrO_4^{2-} unit. Consequently, the bond order within CrO_4^{2-} is smaller than that for CrO_3 in $\text{Cr}_2\text{O}_7^{2-}$, while the bond strength shows the opposite behaviour. The above increase in the stretching frequencies of the Cr=O is therefore essentially caused by a decrease in the negative charge available per Cr^{6+} unit.

The band at 1025 cm^{-1} might correspond to two-fold coordinatively unsaturated sites on amorphous chromia [10] and might contribute to the adsorption of CO_2 on the catalytic surface under ambient conditions. Broad absorptions between 700 and 800 cm^{-1} in both fresh and calcined samples are partly attributed to the bending modes of residual surface hydroxyl groups [27].

Surface rearrangement could have taken place due to the formation of coordinatively unsaturated chromium centres or due to the lowered symmetry of the molecular ions of chromia. It is reported that the decrease in the coordination number of a cation leads to an increase in the frequency of the vibration of the cation-oxygen bond, and hence to an increase in the order of the cation-oxygen bond [28]. Thus, the shift in the frequency of vibration of the chromium-oxygen bond from 950 to 830 cm^{-1} region to 1000 – 1050 cm^{-1} region for the sample calcined at 573 K (Fig. 6b) also suggests that there is a decrease in the coordination number of the chromium cations as a result of calcination. Upon calcination, the effective interaction between the active chromium

phase and the support phase through dehydroxylation results in the formation of the surface chromium species anchored onto the support with a distortion in their tetrahedral symmetry. Evidence for the distortion in the symmetry of surface molecular species can also be had from a diffused band observed around 460 – 400 nm in the visible reflectance spectrum, (Fig. 7b) assigned to a symmetry-forbidden transitions ${}^1\text{T}_1-{}^1\text{A}_1$ (${}^1\text{t}_1-2\text{e}$) of tetrahedral symmetry of CrO_4^{2-} in solution. The fact that the symmetry-forbidden transition of tetrahedral symmetry becomes an allowed transition indicates that a distortion has occurred in the tetrahedral symmetry of CrO_4^{2-} molecular ions as a result of calcination at 573 K for 2 h [9]. The distortion in Td symmetry would also have occurred owing to the formation of dichromate species, which has a lower symmetry than Td [29–31]. UV-VIS-DRS profile also shows a band at 376 nm corresponding to the tetrahedral chromate transitions, confirming the chemical state of chromium to be (VI) even at 573 K [32].

Further evidence for the occurrence of distortion in the symmetry of the molecular ions of chromia as a result of interaction can be had from investigating the effect of calcination on the physical mixture of CrCe 2. Since the calcination was already performed for 2 h on CrCe catalysts, efforts were also made to study the influence of calcination for the physical mixture of CrCe 2 in 1 and 1.5 h of time duration. The DRS profile shown in Fig. 7a of the sample calcined at 573 K for 1 h shows the bands at 290 , 375 nm and a broad band between 420 and 550 nm attributed to the forbidden charge transfer transitions of CrO_4^{2-} ion. The broad band evolving between 420 and 550 nm after calcination for 1 h is due to the chromia species in good interaction with the support phase accompanying the dispersion of CrO_3 on the support surface. It is also observed that, with the increase in duration of calcination from 1 to 1.5 h, the band becomes less pronounced. The same can be ascribed to the provoking of sintering of the previously dispersed CrO_3 phase and/or the formation of chromium species in lower than Cr^{6+} oxidation states. The suppression of bands at 290 and 375 nm with calcination time supports the view that calcination would have reduced the free or non-anchored chromium species preferentially, as anchoring is limited to certain definite sites on the support surface [33].

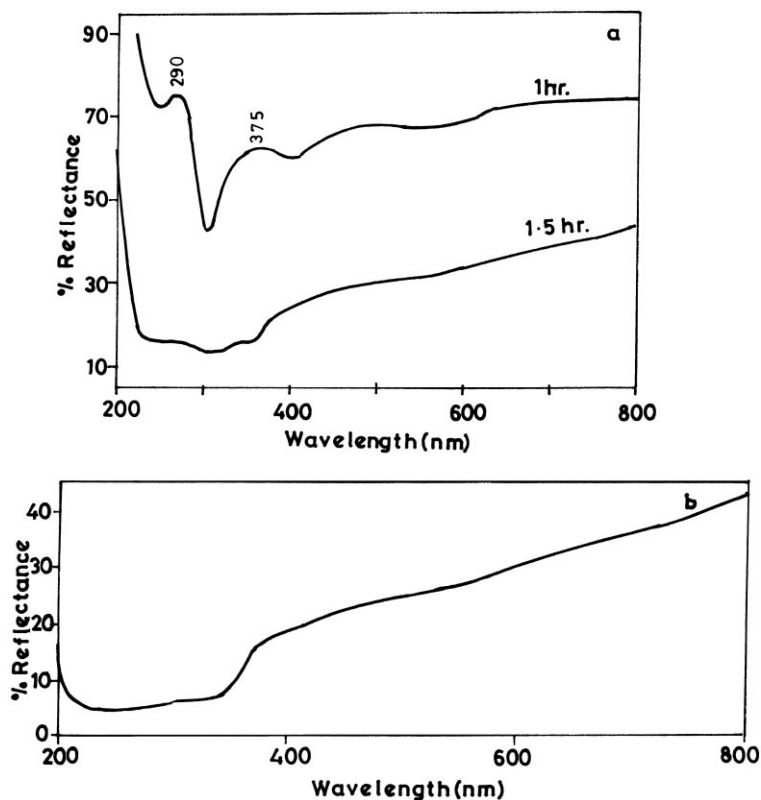


Fig. 7. (a) UV-VIS-DRS profiles of CrCe 2 physical mixture, calcined at 573 K; (b) UV-VIS-DRS profile of CrCe 2, calcined at 573 K, 2 h.

Calcination studies were also carried out using in situ FTIR for CrCe 10 with the aim to compare the behaviour of molecular states of chromia under ambient conditions. Results are shown in Fig. 8. It is observed that the bands in the $830\text{--}960\text{ cm}^{-1}$ are not found to be shifting towards higher frequency region, at least under the conditions employed in the above study. The bands in this region becomes less significant with the increase in calcination temperature from room temperature to 373 K and with the further increase in temperature to 423 K it disappears, indicating the growth of Cr^{3+} as a result of decomposition [34]. However, based on the above observation alone, it cannot be concluded that the interaction between CrO_3 and the support is absent. It is possible that, since the study was carried out under a vacuum of the order of 10^{-6} Torr, the interaction would have taken place between the calcination temperature of 373 and 423 K for which the spectrum was not recorded. The other possible explanation can be that chromium and

cerium ions undergo surface reduction under vacuum [33] and, hence, the prior reduction of these surface species would have taken place even before getting anchored on to the support.

UV-VIS diffuse reflectance spectroscopic studies have been carried out for bulk Cr_2O_3 . The bands observed around 412, 535 nm in the visible region of DRS [24] for the bulk Cr_2O_3 are attributed to ${}^4\text{T}_{2g}$, ${}^4\text{T}_{1g}$, $\leftarrow {}^4\text{A}_{2g}$ transitions typical of Cr^{3+} in Cr_2O_3 , assuming octahedral coordination [29].

The FTIR spectrum for CrCe 10 calcined in air at 673 K for 2 h is shown in Fig. 6c. The absence of bands at 1033 , 1018 , 1004 cm^{-1} and between 950 and 830 cm^{-1} region indicates the increase of Cr^{3+} species [27]. Moreover, at this temperature the physical appearance of the sample becomes greenish, showing the presence of Cr^{3+} species in either amorphous or crystalline form. DRS profile of the above sample shows bands in the visible region around 412 and 535 nm characteristic of Cr^{3+} of pure Cr_2O_3 (Fig. 9). The

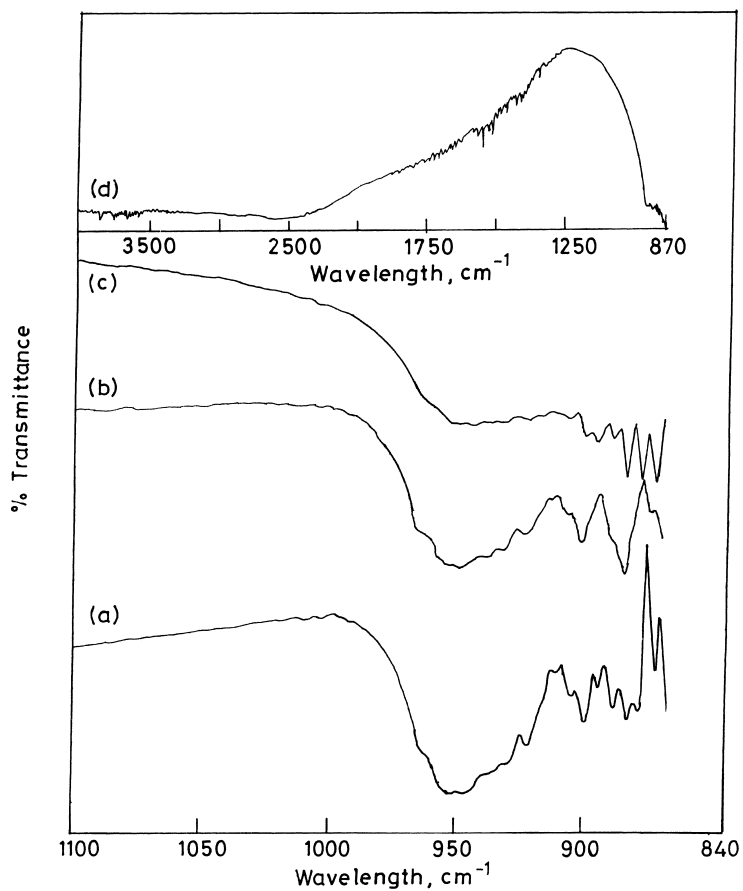


Fig. 8. FTIR spectra of CrCe 10 under in situ conditions as a function of temperature: (a) at 303 K, 2.2×10^{-6} Torr, 15 min; (b) at 323 K, 4.6×10^{-6} Torr, 15 min; (c) at 373 K, 5.5×10^{-6} Torr, 15 min; (d) at 423 K, 9.6×10^{-6} Torr, 15 min.

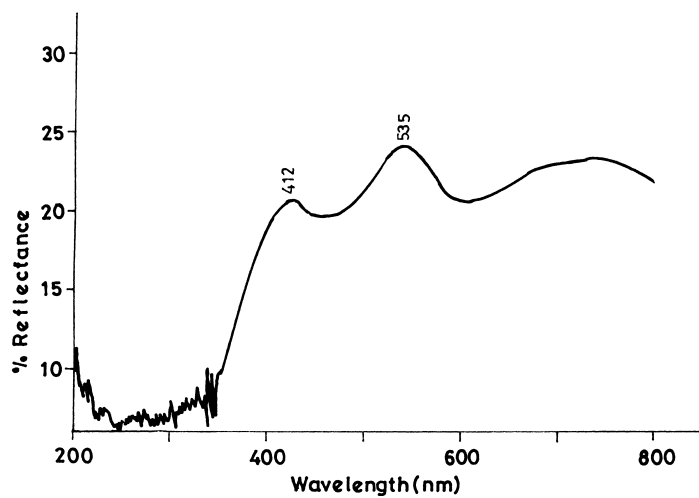


Fig. 9. UV-VIS-DRS profile of CrCe 10, calcined at 673 K, 2 h.

powder XRD pattern for the above sample does not show any detectable Cr_2O_3 phase, confirming the presence of amorphous or microcrystalline Cr^{3+} species. Thus, it is clear that XRD only detects compounds having sufficiently well-developed crystallinity (greater than 40 Å), whereas DRS detects both crystalline and amorphous or molecular-type species. Hence, the combination of the two techniques provide complementary information.

4. Conclusions

The chemical analysis carried out for the CrCe 5 sample reveals the distribution of different types of chromia species present on the ceria surface. The chromium is distributed as free (7.7%) and anchored Cr^{6+} (56%) species as well as Cr^{3+} species (20%), which includes isolated and amorphous Cr^{3+} along with the small amount of crystalline Cr_2O_3 .

The absence of chromia (CrO_3) phase in the diffraction pattern for the supported catalysts when compared to the bulk chromia even at higher temperatures and chromia content, suggests that the chromium species are randomly dispersed, disordered and the crystalline size may be smaller than the detection limit.

The deposition of chromium species on CeO_2 support causes the plugging of pores on the support by chromia phase, as is evident from the decrease in surface area and the pore volume for the chromium-loaded samples.

EGA results confirm the formation of anchored surface chromium species due to the effective interaction between the chromia and the support phase through dehydroxylation. Moreover, the presence of surface heterogeneity after loading chromia over ceria is substantiated by the desorption of CO_2 at multiple temperatures due to the presence of coordinatively unsaturated chromium sites which adsorb CO_2 as carbonate-like species in more than two forms.

EGA and NIR DRS results suggest that the interaction between the support and the active phase decreases when the chromia content crosses the 4–5 wt.% range, owing to the growth of bulk chromia.

FTIR and DRS study indicates the occurrence of a surface rearrangement of the molecular chromium species on the support with the calcination temperature. Surface rearrangement could have taken place

through the change in coordination and chemical environment or through the lowering of tetrahedral symmetry of molecular states of chromium as a result of interaction between the support and the active phase. Both the spectroscopic results agree with the stabilisation of Cr^{6+} species on the ceria support even at 573 K.

FTIR spectra confirm the presence of CO_2 on the catalytic surface and also support the view that coordinatively unsaturated chromium sites are responsible for the adsorption of weakly and strongly adsorbed CO_2 as carbonates. In situ FTIR measurements carried out for CrCe 10 indicates that surface reduction of chromium and cerium has probably taken place under the conditions employed.

The DRS results also support the view that after calcination at 573 K for 2 h, the tetrahedral symmetry of the surface molecular states of chromium gets perturbed as a result of anchoring through dehydroxylation. The colour of the sample and the appearance of the bands corresponding to chromium (III) species, assuming octahedral coordination in the visible region of the reflectance spectrum for the sample calcined at 673 K, implies the formation of Cr_2O_3 as X-ray amorphous microcrystals. Thus, the combination of both DRS and XRD provides complementary information as XRD detects only crystals of sufficiently well-developed crystallinity.

Acknowledgements

The author acknowledges the Council of Scientific and Industrial Research (CSIR), New Delhi, for funding a research project. One of the authors (PW) sincerely expresses his gratitude to Prof. B. Viswanathan for elucidating discussions throughout the course of this investigation. He also thanks Miss A. Mahajabeen (Junior Research Fellow) for her skillful assistance in the present work.

References

- [1] F.D. Hard castle, I.E. Wachs, *J. Mol. Catal.* 46 (1988) 173.
- [2] M. Jehng, A.M. Turek, I.E. Wachs, *Appl. Catal. A. Gen.* 83 (1992) 179.
- [3] J. Engweiler, J. Nickl, A. Baiker, K. Kohler, C.W. Schlappfer, A. von Zelewsky, *J. Catal.* 145 (1994) 141.

- [4] J.P. Hogan, *J. Polym. Sci. Part A-1* 8 (1970) 2637.
- [5] Ch. Fountzoula, H.K. Matralis, Ch. Papadopoulou, G.A. Voyiatzis, Ch. Kordulis, *J. Catal.* 172 (1997) 391.
- [6] B.M. Weckhuysen, I.E. Wachs, R.A. Schoonheydt, *Chem. Rev.* 96 (1996) 3327.
- [7] G. Deo, I.E. Wachs, *J. Phys. Chem.* 95 (1991) 5889.
- [8] F. Cavani, M. Koutyrev, F. Trifiro, A. Bartolini, D. Ghisletti, R. Iezzi, A. Santucci, G.D. Piero, *J. Catal.* 158 (1996) 236.
- [9] B.M. Weckhuysen, A.A. Verberckmoes, A.L. Buttiens, R.A. Schoonheydt, *J. Phys. Chem.* 98 (1994) 579.
- [10] P. Ratnasamy, J. Leonard, *J. Phys. Chem.* 96 (1972) 5008.
- [11] W. Hill, G. Ohlmann, *React. Kinet. Catal. Lett.* 38 (1989) 289.
- [12] V.J. Ruddick, P.W. Dyer, G. Bell, U.C. Gibson, P.S. Badyal, *J. Phys. Chem.* 100 (1996) 11062.
- [13] G. Ghiotti, A. Chiorino, F. Boccuzzi, *Surf. Sci.* 251/252 (1991) 1100.
- [14] P.A. Chernavskii, V.V. Lunin, *Kinet. Catal.* 34 (1993) 470.
- [15] S. Kacimi, J. Barbier Jr., R. Taha, D. Duprez, *Catal. Lett.* 22 (1993) 343.
- [16] F. Roozeboom, M.C. Mittelmeijer-Hazeleger, J.A. Moulijn, J. Medema, V.H.J. de Beer, P.J. Gellings, *J. Phys. Chem.* 84 (1980) 2783.
- [17] J.C. Summers, S.A. Ausen, *J. Catal.* 58 (1979) 131.
- [18] A. Badri, C. Binet, J.C. Lavalley, *J. Chem. Soc., Faraday Trans.* 92 (1996) 1603.
- [19] J. Barrault, A. Alouche, V.P. Boncour, L. Hilaire, A.P. Guegan, *Appl. Catal. A. Gen.* 46 (1989) 269.
- [20] A. Trovarelli, C. de Leitenburg, M. Boara, G. Dolcetti, *Catal. Today* 50 (1999) 353.
- [21] F. Bozon Verduraz, A. Bentaleem, *J. Chem. Soc., Faraday Trans.* 90 (1994) 653.
- [22] P. Moriceau, B. Grzybowska, Y. Barboux, G. Wrobel, G. Hecquet, *Appl. Catal. A. Gen.* 168 (1998) 269.
- [23] S. Haukka, *Analyst* 116 (1991) 1055.
- [24] R.P. Viswanath, P. Wilson, P. Madhusudhan Rao, A. Mahajabeen, in: V. Murugesan, B. Arabindoo, M. Palanichamy (Eds.), *Recent Trends in Catalysis*, Narosa Publications, India, 1999, p. 142.
- [25] C.G. Barraclough, J. Lewis, R.S. Nyholm, *J. Chem. Soc.* (1959) 3552.
- [26] W.E. Hobbs, *J. Chem. Phys.* 28 (1958) 1220.
- [27] A. Zecchina, S. Coluccia, L. Cerruti, E. Borello, *J. Phys. Chem.* 75 (1971) 2783.
- [28] A.A. Davydov, Yu.M. Shchekochikhin, N.P. Keier, A.P. Zeif, *Kinet. Catal.* 10 (1969) 919.
- [29] C.P. Poole, J.F. Itzel, *J. Chem. Phys.* 39 (1963) 3445.
- [30] A. Iannibello, S. Marengo, P. Tittarelli, G. Morelli, A. Zecchina, *J. Chem. Soc., Faraday Trans.* 1 80 (1984) 2209.
- [31] Z.G. Szabo, K. Kamaras, Sz. Szebeni, I. Ruff, *Spectrochim. Acta* 34A (1978) 607.
- [32] B.M. Weckhuysen, B. Schoofs, R.A. Schoonheydt, *J. Chem. Soc., Faraday Trans.* 93 (1997) 2117.
- [33] L.G. Fierro, J. Soria, J. Sanz, M. Rojo, *J. Solid State Chem.* 66 (1987) 154.
- [34] N.E. Fouad, H. Knozinger, *Z. Phys. Chem.* 171 (1991) 75.